Flow Survey of the Vortex Wake behind Wings

Z. El-Ramly* and W. J. Rainbird†
Carleton University, Ottawa, Canada

Flowfield surveys of the wake behind three different wings have been carried out in a low-speed wind tunnel. The mean flow properties have been measured using a small non-nulling five-hole probe. The results include the three mean velocity components, complete definition of the viscous wake, and detailed loading on one of the wings. The three components of vorticity were calculated and the vortical wake completely defined. It was found that the vortical wake always is contained within the viscous wake (region of total pressure loss). The vortex system is never fully rolled up, in the traditional sense, within the reasonably large downstream distance tested of 13 wing spans. The overall lift coefficient calculated from the distribution of streamwise component of vorticity is found to be smaller (87-100%) than that measured directly on the wing. The total circulation accounted for, at any streamwise station, decreases slightly with downstream distance. Comparison was made between the measured tangential velocity profiles and circulation distribution and those calculated using Betz theory, based on measured spanwise loading. Agreement is reasonable over a radius more or less equal to that of the vortex viscous core ($<0.25\ b/2$). Outside of this region, the Betz model assumes that roll-up is complete when, in fact, it is not. Agreement is also poor very near the vortex center because of the strong viscous effects there.

Introduction

THE problem of aircraft trailing vortices and their effect on flight safety and airport capacity has generated interest and concern in recent years (see, for example, Refs. 1-3 for surveys of the problem). However, concentrated efforts aimed at alleviating the problem have met with only limited success, as is clear from the latest NASA Symposium on Wake Vortex Minimization.[4] Some significant alleviation has been obtained; unfortunately, the concepts for doing so carry heavy penalties in other areas of airplane performance. Nevertheless, some investigators are calling for more relaxed separation criteria[5,6] or for adaptive separation, assisted by vortex tracking sensors and/or meteorological sensors to determine safe reduced spacing. Of course, any wake-vortex avoidance strategy relies on the ability to predict vortex formation, transport, and decay. Unfortunately, theoretical models of these processes have not been developed yet to an acceptable level. Most of the existing predictive schemes[3,7,8] are based on the Betz model, as highlighted by Donaldson[9] in recent years. The Betz theory uses the laws of conservation of momentum in "potential" flow to relate the structure of the vortex sheet behind an isolated wing to the structure of a single, fully developed vortex. Even though there are some limited systematic comparisons with the Betz theory,[10] the associated measurements were made in the very near field ($<1.25\ b$) where the vortex system is not expected to be fully rolled up. More systematic comparison with models based on Betz's theory and examination of the validity of the conservation laws applied are needed.

Aircraft trailing vortices do not lend themselves easily to laboratory investigation, the main problem being limitations on available downstream distance and the usual difficulties with Reynolds number simulation giving distorted relative scale of viscous region of the flow. Another obvious problem is wall interference, although this can be accounted for approximately.[11] Attempts to increase the available downstream distance using small wings in the large NASA Ames 40- × 80-ft wind tunnel[12,13] resulted in a distorted vortex path (vortex meander) with associated measuring problems and of course did not help with Reynolds number simulation. In most wind-tunnel tests,[14-19] the vortex is assumed to be axisymmetric, and hence only limited scans through the vortex centers are made. Measurements made by the present authors[20-24] and by deVries[25] show that, for distances of at least five spans behind a sweptback wing, the vortex is not fully rolled up and not axisymmetric. This means that detailed flow surveys must be made in order to define the flowfield fully. It also is important to extend these measurements further downstream and to confirm the findings behind wings of different configuration.

In this paper, detailed flowfield surveys of the vortex system behind different wings of three different configurations are presented. The flowfield is mapped using a very small non-nulling five-hole probe that is finely scanned behind the wings at several axial (downstream) stations. The results include the three components of mean velocity, the three components of vorticity, the total pressure loss coefficient, and contours of equal total pressure loss and of equal streamwise component of vorticity. For one wing, detailed chordwise and spanwise loadings are obtained from surface pressure distributions. For the other two wings, overall lift and drag characteristics are measured using an overhead balance system.

The main emphasis of this paper is on correlating the data from the three wings and on comparisons with available roll-up models (in particular those related to the Betz roll-up theory) rather than on presentation of the detailed results themselves. The relation between the vortical and viscous wakes also is examined carefully.

Experimental Setup

The tests were carried out in the Carleton University 20- × 30-in. low-speed return circuit wind tunnel with an extended-length test section. The axial pressure gradient along the test section is essentially zero, and the flow quality is very good (spatial variation of mean flow angularity within ±0.15° and streamwise component of turbulence approximately 0.1%). Complete details of the setup can be found in Refs. 20 and 21. The facility is fully computer controlled, with on-line data reduction and plotting; this made the detailed mapping of the flowfield feasible. Details of the computer and control system can be found in Ref. 23.

Presented as Paper 77-175 at the AIAA 15th Aerospace Sciences Meeting, Los Angeles, Calif., Jan. 24-26, 1977; submitted Jan. 28, 1977; revision received June 2, 1977.

Index categories: Testing, Flight and Ground; Jets, Wakes, and Viscid-Inviscid Flow Interactions.

*Senior Research Associate, Department of Mechanical and Aeronautical Engineering. Member AIAA.

†Professor of Engineering, Department of Mechanical and Aeronautical Engineering. Member AIAA.

Table 1 Main dimensions of generating wings

	Main (half) wing	Swept Wing	Rectangular Wing
Aspect Ratio	7.0	8.5	3.96
Span (inches)	21.0 (42.0)	20.0	16.40
Sweepback Angle ($\frac{1}{4}c$)	35°	25°	0°
Taper Ratio	3.0	3.0	1
Root Chord (inches)	9.0	3.51	4.16
Tip Chord (inches)	3.0	1.17	4.16
Wing Section	ONERA Peaky	NACA 64_2-015	Symmetrical
Thickness (symmetrical)	12 %	15 %	8 %
Equivalent Distance Downstream (from ¼ chord point to mean chord of generating wing)			
Station 1	$1.7\bar{c}$(0.35b)	0.3b	0.35b
Station 2	2.5b	5.4b	6.5b
Station 3	5.0b	10.5b	13.0b

Table 1 gives the overall dimensions of the wings used, whereas Fig. 1 is a sketch of these wings. The main wing (a half-wing) was mounted on an incidence gear on the 20-in. sidewall of the working section; provision was made for sidewall boundary-layer suction.[21,23] The smaller wings were supported in the center of the working section by a single strut attached to the overhead balance. Care has been taken in fixing transition near the leading edge of both surfaces of the wings because of the relatively low Reynolds number of the tests (0.26 to 0.51×10^6 based on mean chord). A surface flow visualization technique, using oil dots, was used to check the approximate nature of the boundary layer on the wings.

Flowfield measurements were made at three downstream stations behind each wing. The position of the first station was chosen to be at a constant 1.7 chords downstream of the trailing edge of the main wing. The third station is near the test section exit and is equivalent to 13 spans downstream of the smallest wing. Table 1 also gives the equivalent downstream distance, in spans of the vortex generating wing, for the three stations.

Since the velocity measurements were to be used in calculating the vorticity and circulation distribution, and these are sensitive to the accuracy of the measurements, special care was required in performing the experiment. Basic nonuniformities of the flowfield, probe misalignment, and upstream effects of the traversing mechanism all were accounted for. This was achieved by making separate traverses at each measuring station, with the generating wing removed from its position near the upstream end of the extended working section. More details of the probe calibration, empty tunnel correction, and accuracy of the measurements can be found in Ref. 23.

Results and Discussion

The overall lifting characteristics of the wings are given in Fig. 2. For the main wing, the lift coefficient was obtained from a double integration of the pressure distributions, whereas the lift characteristics of the two other wings were measured directly on a three-component overhead external balance. No angle of incidence corrections to allow for wall or strut interference effects have been applied to the data presented. Flowfield measurements were made at four lift

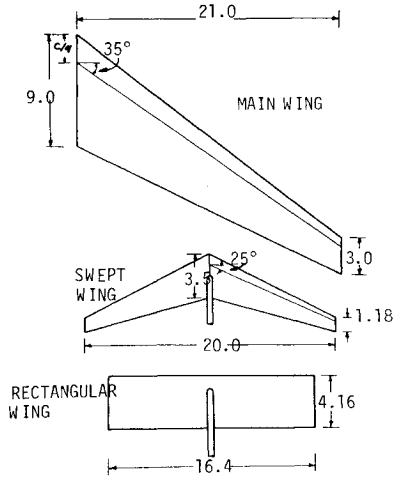

Fig. 1 Sketches of generating wings (dimensions in inches).

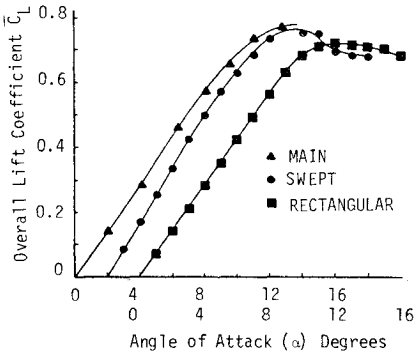

Fig. 2 Lifting characteristics of wings.

coefficients behind the main wing: $\bar{C}_L = 0.36$, 0.58, 0.74, and 0.77 ($\alpha = 5°$, 8°, 11°, and 12.8°); some of these data were published earlier.[21-24] For the two other wings, measurements were made at a negative angle of attack, $\alpha = -7°$, $\bar{C}_L$ about -0.52, so that the strut is effectively on the aerodynamic lower surface, thus minimizing strut interference. This lift coefficient is within the linear range of the lifting characteristics of both wings.

Figure 3 shows the spanwise loading, on the main wing, for the four angles of incidence considered. These loadings have been obtained from pressure distribution data. At higher incidence, progressive "tip stall" resulting from flow separation, first along the streamwise tip and then along the outboard part of the leading edge, unloads the outboard sections and transfers the load toward the root. (A more detailed discussion of the wing loading can be found in Refs. 20 and 21.) The figure also shows the curves (polynominals) fitted to the spanwise data; these polynominals are used in the Betz-type calculation, which will be presented in the next section.

Some sample flowfield results are displayed in Figs. 4 and 5. Figures 4a-4c show selected contours of equal total pressure loss coefficient, whereas Figs. 5a-5c show the corresponding contours of equal streamwise component of vorticity. For the main wing, Fig. 4a shows part of the test section wall boundary layer. The region of the wing wake/wall boundary layer interaction is very small ($< 0.05\ b/2$), indicating that the wing root suction system is working properly. The large difference in the flowfield, near the tip, between $\alpha = 11°$ and 12.8° (Figs. 4a and 5a) is due to extensive leading-edge separation near the tip (over about $0.3\ b/2$) for the $\alpha = 12.8°$ case, as is clear from surface flow visualization. The $\alpha = 12.8°$ case is interesting and is presented here because it represents the behavior of an already diffuse vortex. For the swept and

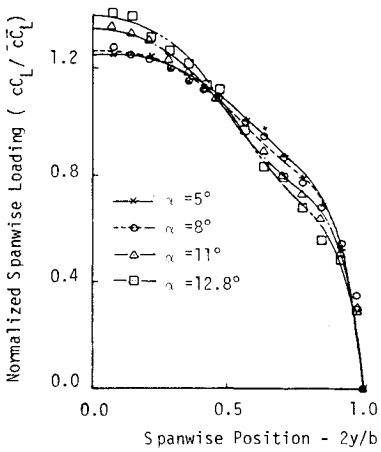

Fig. 3 Spanwise loading of main half-wing.

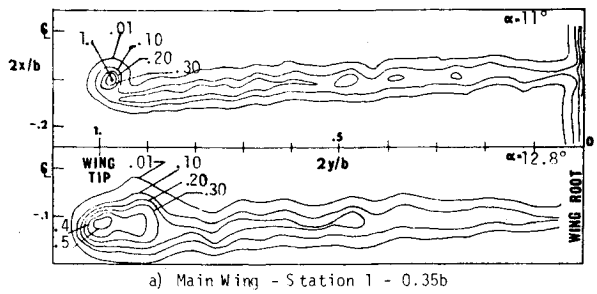

a) Main Wing - Station 1 - 0.35b

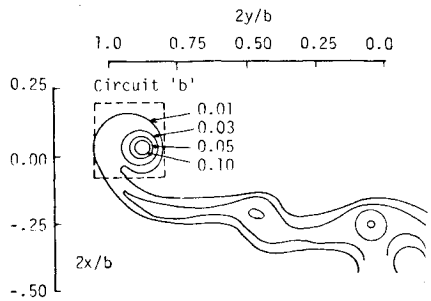

b) Swept Wing - Station 2 - 5.4b

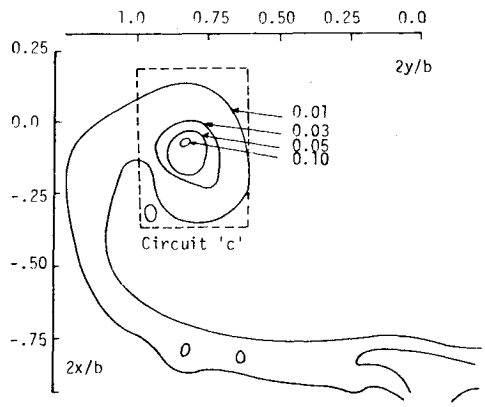

c) Rectangular Wing - Station 3 - 13b

Fig. 4 Contours of equal total pressure loss coefficient, $(P_{0_\infty} - P_0)/\frac{1}{2}\rho V^2_\infty$.

rectangular wing cases (Figs. 4b and 4c), part of the strut wake is apparent. Again strut interference is very small, as is also clear from the contours of equal streamwise component of vorticity, Figs. 5b and 5c. Notice that these wings were tested at negative incidence; however, the axes on the figures are inverted to avoid confusion.

The similarity between contours of equal total pressure loss and those of streamwise component of vorticity is quite obvious. Further examples of vorticity contours are presented

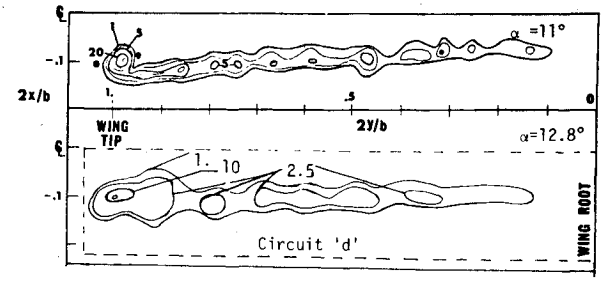

a) Main Wing - Station 1 - 0.35b

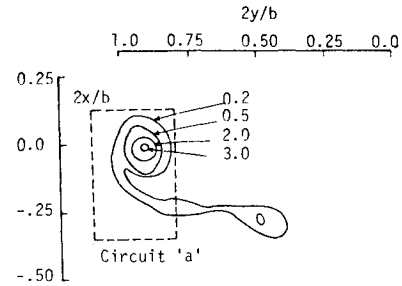

b) Swept Wing - Station 2 - 5.4b

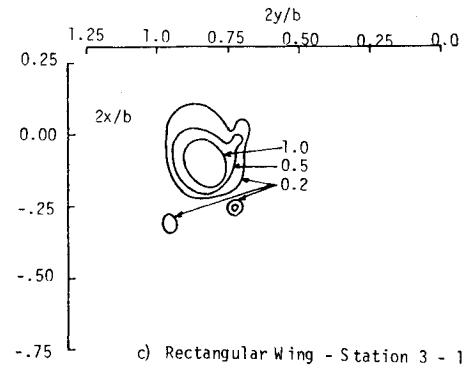

c) Rectangular Wing - Station 3 - 13b

Fig. 5 Contours of equal streamwise component of vorticity, $\zeta b/2V_\infty$.

in Fig. 6; the edge of the viscous wake (defined arbitrarily, but in a manner similar to boundary layers, by the 1% total pressure loss contour) also is outlined on the figure. It is clear that, as should be expected, the vortical wake is completely contained within the viscous wake, and regions of high total pressure loss (the "core") also are associated with high streamwise vorticity. The center of the wake from the vorticity distribution is, however, somewhat above (toward the aerodynamic upper surface of the wing) the center of the wake from the total pressure loss. These conclusions are in agreement with deVries[25] measurements, which were limited to about one span behind a swept nontapered wing.

Another feature of the flow which is displayed in Figs. 5 and 6 is the fact that the vortex system is not fully rolled up, even at station 3, at least for the two swept wings. Some remnant of streamwise vorticity is still visible outside the region of concentrated vorticity (or high total pressure loss) which is treated as the vortex core. The circulation around several specific circuits enclosing the vortex core (defined in Figs. 4b, 4c, and 5c) and also around half the wing was calculated and is given in Table 2. This circulation is normalized by the value derived from the corresponding spanwise loading Γ_r for the main wing, and to the circulation around half the wing Γ_{r_1} (root circulation, circuit *d*), at station 1, for the swept and rectangular wings. The circulation around the vortex core (the nearly axisymmetric part of the flow, circuit *c*) is less than 60% of the root circulation for the swept wings and less than 80% for the rectangular wing. The higher concentration for the rectangular wing is, of course, related to the higher loading near the tips, as will be discussed later.

Table 2 Circulation distribution around different circuits

Wing	α	$\bar{C}_L$	$\frac{2\Gamma_o}{bV_\infty}$	Γ/Γ_o Station 1 Circuit a	Station 1 Circuit b	Station 2 Circuit a	Station 2 Circuit b	Station 2 Circuit c	Station 3 Circuit a	Station 3 Circuit b	Station 3 Circuit c	From V_θ Distribution at Station 3
Main	5°	0.36	1.35	0.36	0.34	0.56	0.51	0.49	0.57	0.51	0.48	0.525
(Half-)Wing	8°	0.57	2.18	0.37	0.34	0.62	0.54	-	0.69	0.62	-	0.58
	11°	0.74	2.96	0.35	0.29	0.55	0.52	-	0.66	0.56	-	0.56
	12.8°	0.77	3.21	0.50	-	0.59	-	-	0.80	0.58	-	0.58
Rectangular Wing		0.52	0.69	0.67	0.63	0.86	0.84	0.79	-	-	0.77	
Swept Wing		0.52	1.18	0.36	-	0.6	0.55	0.52	0.63	0.58	0.54	

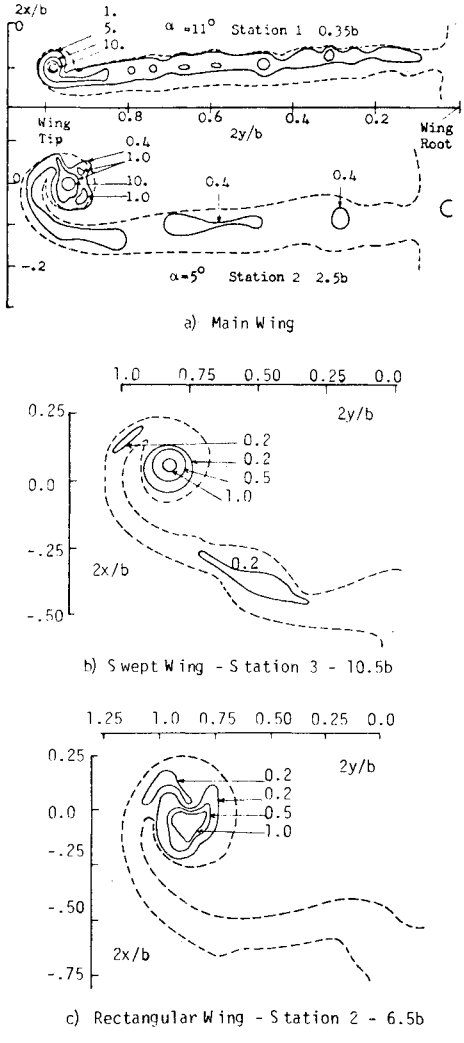

Fig. 6 Comparison of vortical and viscous wakes [solid lines, vorticity contours; broken line, edge of viscous wake (contour of 1% total pressure loss)].

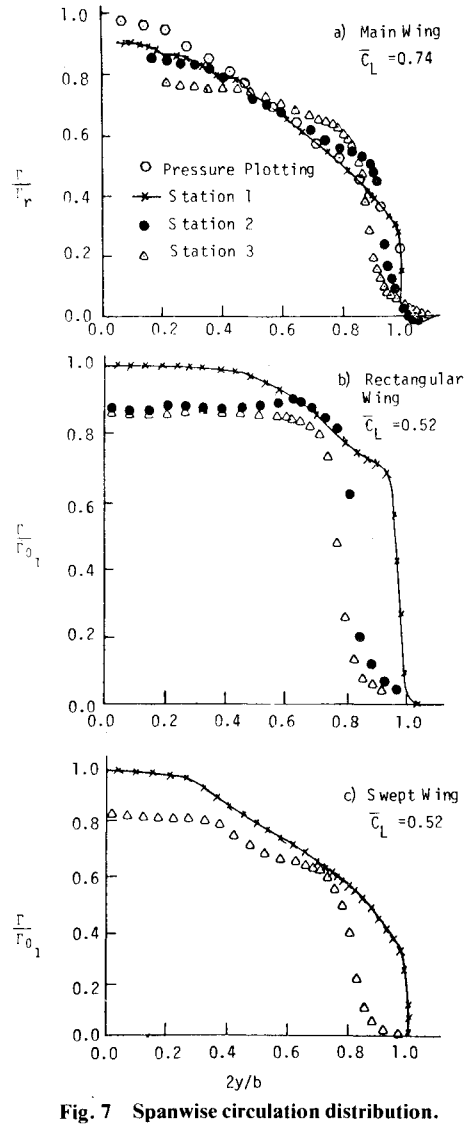

Fig. 7 Spanwise circulation distribution.

References 14, 15, 25, and 26 also reported that less than 60% of the root circulation was measured around the vortex core; this was attributed by other investigators[9] to the failure to extend the measurements far enough away from the vortex core. However, in the present measurements, the remainder of the circulation can be accounted for and is, in fact, found in an unrolled-up layer. Moreover, the small rate of roll-up (increase in core circulation circuit *c*) between stations 2 and 3 suggests that the roll-up is effectively complete, although the vorticity is not necessarily in an axisymmetrical form.

Figure 7 is constructed to account for the remainder of the shed vorticity. This figure shows the spanwise distribution of circulation in the wake, where Γ is calculated by summing up the circulation about vertical strips of the wake extending above and below the viscous region and starting from out-

Table 3 Circulation decay and comparison of measured and calculated lift coefficient

	α	$\bar{C}_L$	$\frac{2\Gamma_r}{bV_\infty}$	$\frac{2\Gamma_o}{bV_\infty}$	C_{L_f}	$\frac{C_{L_f}}{\bar{C}_L}$	$\frac{\Gamma_o}{\Gamma_r}$	$\frac{\Gamma_o}{\Gamma_r}$	$\frac{\Gamma_o}{\Gamma_r}$
	From Loading			Flow Field - Station 1				Station 2	Station 3
Main	5	0.36	1.35	1.24	0.32	0.89	0.92	0.88	0.84
Half-Wing	8	0.58	2.18	2.00	0.53	0.92	0.91	0.90	0.82
	11	0.74	2.96	2.81	0.71	0.96	0.95	0.86	
	12.8	0.77	3.21	3.25	0.78	1.01	1.01	0.98	
Swept Wing	7	0.52		0.69	0.45	0.88	1 [a]		0.84 [a]
Rectangular Wing	7	0.53		1.18	0.49	0.93	1 [a]	0.83 [a]	0.78 [a]

[a] Γ_0 at station 1 is substituted for Γ_r.

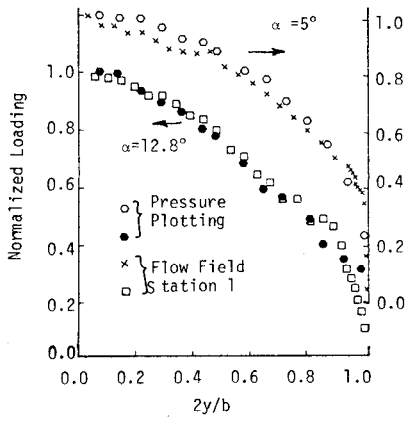

Fig. 8 Comparison of measured and calculated wing loading: main wing.

board of the wing tip and proceeding all the way in to the wing root. Also presented in Fig. 7a is the spanwise load distribution as calculated from detailed surface pressure plotting for the main wing only. The steep rise in circulation appearing in the wing-tip region on Fig. 7 corresponds to crossing and enclosing the vortex center. As is expected, the vortex center drifts inboard as the downstream distance increases.

From the circulation distribution at any downstream station, it is possible to calculate the overall lift coefficient of the generating wing, assuming that the lift impulse is preserved. Table 3 shows the results of these calculations of C_{L_f} at station 1, as well as comparisons with the lift coefficients measured directly by the overhead balance or by pressure plotting. The lift coefficient thus calculated from the flowfield is about 0.88 to 1.01 times that measured directly. It is interesting to notice that the ratio of the calculated to measured lift coefficient is very close to the ratio of the measured (from flowfield) to calculated (from spanwise loading) root circulation.

Figure 8 shows a comparison of the circulation distribution at station 1, normalized to the measured root circulation, and the spanwise loading on the main wing. The shape of the circulation distribution is very similar to the loading on the wing, indicating very little roll-up. Also it is possible to recover or construct the wing loading from flowfield measurements taken close to the trailing edge, if allowance is made for the difference in root circulation. Applying this argument to the swept and rectangular wings (for which no direct measurements of loading are available), we can estimate the root circulation and use it, together with the circulation distribution at station 1, to construct the spanwise loading.

The measured circulation around the rolled-up vortex core (by the core, we mean that portion of the wake which is concentrated in a nearly axisymmetric form, circuit c) is equal to the circulation around a certain wing chordwise section, A, say. According to Stokes' theorem, and assuming the roll-up to proceed uniformly so that the vorticity shed at the tip ends up in the core center, then the vorticity shed outboard of section A will form the core. For the main wing, and from the flowfield measurements at station 3, section A corresponds to 0.1, 0.2, 0.24, and 0.32 semispans or to 0.7, 1.4, 1.68, and 2.24 tip chords from the tips for $\alpha = 5°$, 8°, 11°, and 12.8°, respectively. It is interesting to notice that, for $\alpha = 12.8°$, for example, a relatively higher percentage of the root circulation is measured around the core (0.58 vs 0.48 for $\alpha = 5°$, 5 b downstream, Table 2), even though for $\alpha = 12.8°$ relatively less load is concentrated near the tip as a result of the tip stall, as seen in Fig. 3. However, as a result of the tip stall (with some leading-edge separation), the separated boundary layers are more effective in concentrating the vorticity shed from a larger fraction of the span into the tip vortex; the vortex sheet (free shear layer) already has, in effect, a partially rolled-up shape right where it is shed from the wing. The same argument applies to other angles of attack, as is clear from the trend of the position of section A. For the smaller swept wing with $\bar{C}_L = 0.52$, section A corresponds to 0.10 semispans or 0.85 tip chords from the tip for the results at 10.5 spans downstream. For the rectangular wing A, also at $\bar{C}_L = 0.52$, is at 0.2 semispans or 0.4 tip chords from the tip, for the results at 13 spans downstream. The higher concentration of vorticity in the core for the rectangular wing is simply the result of higher loading near the tip, in agreement with all inviscid analysis. It is suggested that the roll-up develops as follows. A tip vortex is rolled up above the wing upper surface near the tip, in a way analagous to that on slender delta wings with sharp leading edge. The strength of this tip vortex depends on the spanwise load distribution or, more specifically, on rapid variation of local loading near the tip and on the nature of the boundary-layer separation near and at the tip. At the tip trailing edge, a substantial fraction of all of the trailing vorticity (see Table 2, station 1 results, and Refs. 25 and 26) already is concentrated in a tip vortex. The part of the trailing

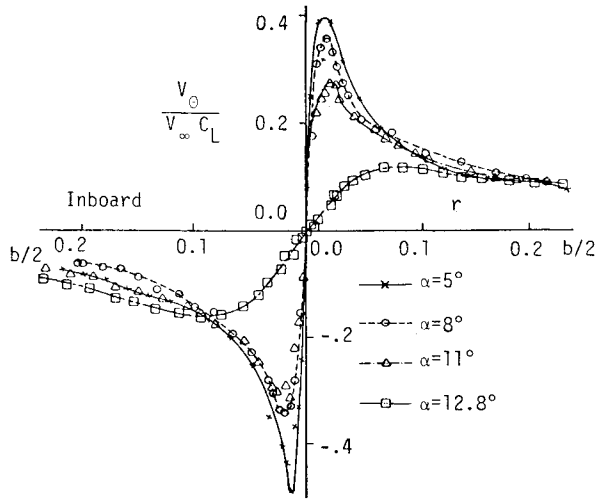

Fig. 9 Measured tangential velocity profiles: main wing, station 3, 5*b*.

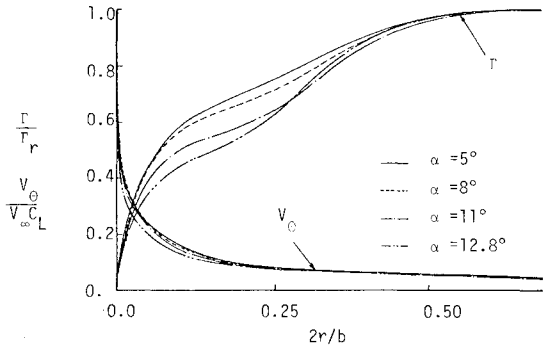

Fig. 10 Betz circulation and velocity distribution: main wing.

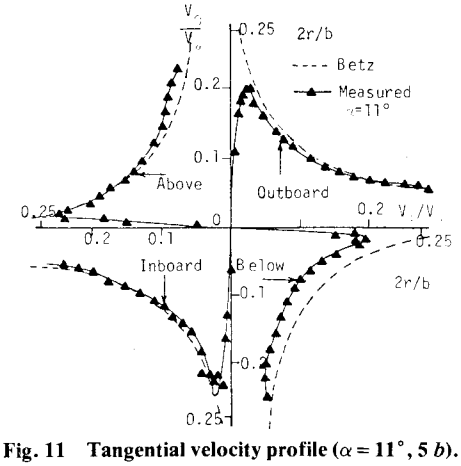

Fig. 11 Tangential velocity profile ($\alpha = 11°$, 5 *b*).

vorticity not concentrated in the tip vortex leaves the wing trailing edge in the form of a free shear layer (vorticity layer). However, because this shear layer has a finite thickness dependent on chord Reynolds number and diffuses as it trails downstream, the roll-up does not proceed as fast as would be predicted from inviscid analysis (assuming the shear layer to be an infinitely thin vortex sheet). In all probability, at least in the light of the results presented, the roll-up at finite Reynolds number is never complete in the traditional sense.

The effect of the nature of the boundary-layer separation near and at the tip on the structure of the vortex core is shown in Fig. 9. The figure shows the tangential velocity distribution, normalized to the overall lift coefficient, at the far downstream station 3. As the angle of attack increases,

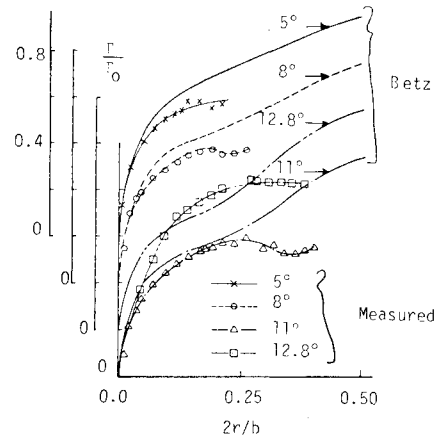

Fig. 12 Comparison of measured circulation with Betz distribution from experimental spanwise loading.

"tip stall" resulting from flow separation, first along the streamwise tip and then along the outboard part of the leading edge (as outlined earlier), extends over a larger fraction of the span. As a result, the vortex core is more diffused; this is reflected in lower tangential velocities near the center, as shown in Fig. 9. Examining Table 3, it is interesting to notice that the best agreement between the flowfield and the directly measured wing loading results is found for $\alpha = 12.8°$, when intuitively it would be least expected because of the large leading edge separation that then occurs near the wing tip. The highest discrepancy is for the case of a fully attached flow, $\alpha = 5°$ and 8°.

Comparison with Betz Model

It is clear from these experiments that the roll-up is not complete and that very little further roll-up is apparent between stations 2 and 3. However, calculations were performed to examine how the structure of the roll-up portion of the vortex in the present experiments compares with the Betz model. The calculations use as input the fitted curves of spanwise loading on the main (half-) wing obtained from the detailed pressure plotting (Fig. 3) and assume a complete or full roll-up. The results of these calculations, which include the circulation and tangential velocity distribution, are shown in Fig. 10. Comparison with Fig. 9 shows that the Betz model overestimates the velocities very near the vortex center, which is expected, since the model does not include any viscous effects, and these are very strong near the vortex center. However, if the vortex has a large core, for example, the $\alpha = 12.8°$ case, the Betz model greatly overestimates the velocities over a large region ($\simeq 0.1\ b/2$). A more detailed comparison is shown in Fig. 11, for $\alpha = 11°$ at the 5 *b* station. The asymmetry of the measured velocity profiles, because of the incomplete roll-up, is very clear. The Betz model still reasonably predicts the tangential velocities over a large region, and this is probably the region of interest to a following aircraft.

The radial distribution of circulation from the flowfield results (such as those presented in Fig. 11) is obtained by averaging the tangential velocity above, below, inboard, and outboard of the vortex center. Comparison of the circulation results with the corresponding Betz results at the 5 *b* station for the main wing is shown in Fig. 12. Agreement is reasonable over a radius more or less equal to that of the vortex core as determined from the total pressure and vorticity results of Figs. 4-6. Outside of this region, the Betz model assumes that roll-up is complete when, in fact, it is not. Notice, however, that this will affect the velocity only far from the vortex center, where it is very small in any case. Completely inviscid models should not, of course, be expected to provide a fully accurate description of the flowfield.

Conclusions

The following conclusions have been drawn from detailed surveys of the flowfield, behind three different wings and up to 13 spans downstream:

1) The vortical wake (region of nonzero vorticity) is contained within the viscous region of the wake.

2) The vortex is never fully rolled up, in the traditional sense, within the measuring range of the experiment. For the rectangular wing, less than 74% of the root circulation is rolled up in a concentrated core; for the swept wings, less than 60% is rolled up. Moreover, the development with downstream distance suggests that no appreciable further roll-up occurs.

3) A qualitative roll-up model has been suggested which relates the strength of the tip vortex to the load distribution near the tip and to the nature of the boundary-layer separation near the tip.

4) The Betz model of roll-up overestimates the tangential velocity and circulation near the vortex center because it does not consider viscous effects. It also overestimates the circulation and tangential velocity far from the vortex core because it does not allow for incomplete roll-up. However, the model provides a good working tool, since it gives reasonable predictions of the flowfield over a range that would be of interest to a smaller following aircraft. In any case, hazard assessment based on the Betz model would be on the conservative side.

Acknowledgments

The authors would like to thank R. J. Kind for revising this paper. This research was supported by the National Research Council of Canada under Grant A7799.

References

[1] Olsen, J., Goldberg, A., and Rogers, M., *Aircraft Wake Turbulence and Its Detection*, Plenum Press, New York, 1971.

[2] El-Ramly, Z., "Aircraft Trailing Vortices: A Survey of the Problem," Carleton Univ., Ottawa, Canada, ME/A 72-1, Nov. 1972.

[3] Donaldson, C. duP. and Bilanin, A., *Vortex Wakes of Conventional Aircraft*, AGARDograph 204, May 1975.

[4] *NASA Symposium on Wake Vortex Minimization*, Washington, D. C., Feb. 25-26, 1976.

[5] Hallock, J. N. and Goldstone, L., "US/UK Vortex Monitoring Program at Heathrow Airport," *AGARD Guidance and Control Panel 20th Symposium on Plans and Developments for Air Traffic Systems*, Paper 24, 1975.

[6] Hallock, J. N., Wood, W. O., and Spitzer, E. A., "Predictive Techniques for Wake Vortex Avoidance," *AGARD Guidance and Control Panel 20th Symposium on Plans and Developments for Air Traffic Systems*, Paper 23, 1975.

[7] Rossow, V. J., "On the Inviscid Roll-Up Structure of Lift Generated Vortices," *Journal of Aircraft*, Vol. 10, Nov. 1973, pp. 647-650.

[8] Bilanin, A. J. and Donaldson, C. duP., "Estimation of Velocities and Roll-Up in Aircraft Vortex Wakes," *Journal of Aircraft*, Vol. 12, July 1975, pp. 578-585.

[9] Donaldson, C. duP., "A Brief Review of the Aircraft Trailing Vortex Problem," Air Force Office of Scientific Research, AFOSR-TR-71-1910. ARAP Rept. 155, May 1971.

[10] Bilanin, A. J., Donaldson, C. duP., and Snedeker, R. S., "An Analytical and Experimental Investigation of the Wake Behind Flapped and Unflapped Wings," Air Force Flight Dynamics Lab., AFFDL-TR-74-90, Sept. 1974.

[11] Mokry, M. and Rainbird, W. J., "Calculation of Vortex Sheet Roll-Up in a Rectangular Wind Tunnel," *Journal of Aircraft*, Vol. 12, Sept. 1975, pp. 750-752.

[12] Corsiglia, V. R., Schwind, R. G., and Chigier, N. A., "Rapid Scanning, Three Dimensional Hot Wire Anemometer Surveys of Wing-Tip Vortices," *Journal of Aircraft*, Vol. 10, Dec. 1973, pp. 752-757.

[13] Rossow, V. J., Corsiglia, V. R., and Phillippe, J. J., "Measurements of the Vortex Wakes of a Subsonic and a Supersonic-Transport Model in the 40- by 80-Foot Wind Tunnel," NASA TMX-62-391, Sept. 1974.

[14] Dosanjh, D. S., Gasparek, E. P., and Eskinazi, S., "Decay of a Viscous Trailing Vortex," *Aeronautical Quarterly*, Vol. 13, May 1962, pp. 167-188.

[15] Grow, T. L., "Effect of Wing on Its Tip Vortex," *Journal of Aircraft*, Vol. 6, Jan.-Feb. 1969, pp. 37-41.

[16] Logan, A. H., "Vortex Velocity Distributions at Large Downstream Distances," *Journal of Aircraft*, Vol. 8, Nov. 1971, pp. 930-932.

[17] Chigier, N. A. and Corsiglia, V. R., "Wind Tunnel Studies of Wing Wake Turbulence," AIAA Paper 72-41, San Diego, Calif., Jan. 1972.

[18] Mason, W. H. and Marchman, J. F., "The Farfield Structure of Aircraft Wake Turbulence," AIAA Paper 72-40, San Diego, Calif., Jan. 1972.

[19] Orloff, K. L., "Trailing Vortex Wind Tunnel Diagnostics with a Laser Velocimeter," *Journal of Aircraft*, Vol. 11, Aug. 1974, pp. 477-482.

[20] El-Ramly, Z. and Rainbird, W. J., "Wind Tunnel Measurements of Rolling Moment in a Sweptback Wing Vortex Wake," *Journal of Aircraft*, Vol. 13, Dec. 1976, pp. 962-967.

[21] El-Ramly, Z., "Investigation of the Development of the Trailing Vortex System Behind a Sweptback Wing," Carleton Univ., Rept. ME/A 75-3, Oct. 1975.

[22] El-Ramly, Z. and Rainbird, W. J., "Effect of Simulated Jet Engine on the Flow Behind a Sweptback Wing," *Journal of Aircraft*, Vol. 14, April 1977, pp. 343-349.

[23] El-Ramly, Z. and Rainbird, W. J., "Computer-Controlled System for the Investigation of the Flow Behind Wings," *Journal of Aircraft*, Vol. 14, July 1977, pp. 668-674.

[24] El-Ramly, Z., "Wind Tunnel Flow Field Measurements Behind a Sweptback Wing," Lockheed Georgia Contractor Rept. P. O. CK27059P, Dept. of Mechanical and Aeronautical Engineering, Carleton Univ., Ottawa, Canada, Feb. 1976.

[25] deVries, O., "Wind Tunnel Investigation of the Development of the Vortex Wake Behind a Sweptback Wing," National Aerospace Lab., The Netherlands, NLR-TR-72017U, March 1973.

[26] Smith, W. G. and Lazzeroni, F. A., "Experimental and Theoretical Study of a Rectangular Wing in a Vortical Wake at Low Speed," NASA TN D-339, Oct. 1960.